Measurement of Contact Behavior Including Slippage of Cuff When Using Wearable Physical Assistant Robot

Yasuhiro Akiyama, Shogo Okamoto, Yoji Yamada, *Member, IEEE*, and Kenji Ishiguro

***Abstract*—Continuous use of wearable robots can cause skin injuries beneath the cuffs of robots. To prevent such injuries, understanding the contact behavior of the cuff is important. Thus far, this contact behavior has not been studied because of the difficulty involved in measuring the slippage under the cuff. In this study, for the first time, the relative displacement, slippage, and interaction force and moment at the thigh cuff of a robot during sit-to-stand motion were measured using an instrumented cuff, which was developed for this purpose. The results indicated that the slippage and relative displacement under the cuff was uneven because of the rotation of the cuff, which suggests that the risk of skin injuries is different at different positions. Especially, the skin closer to the hip showed larger dynamism, with a maximum slippage of approximately 10 mm and a displacement of 20 mm during motion. Another important phenomenon was the individual difference among subjects. During motion, the interaction force, moment, and slippage of some subjects suddenly increased. Such behavior results in stress concentration, which increases the risk of skin injuries. These analyses are intended to understand how skin injuries are caused and to design measures to prevent such injuries.**

***Index Terms*—Physical Assistant Robot, Contact Mechanics, Human–Robot Interaction, Safety.**

I. Introduction

PHYSICAL assistant robots can effectively improve the quality of life of elderly people and increase the productivity of workers, both of which are very important in an aging society. Some existing physical assistant robots have been proven to be useful for rehabilitating stroke patients [1], [2], for making elderly people active [3], and for providing assistance in labor-intensive tasks [4], [5]. In addition, exoskeletons have been developed for various specialized uses such as military applications [6].

Wearable physical assistant robots require a higher level of safety than other robots because of their close contact with the user's body. The contact safety of a physical assistant robot was studied recently [7]. Now, a new ISO standard ISO 13482 [8], which regulates the safety standard of personal care robots, including physical assistant robots, has been launched. According to this standard, a physical assistant robot should ensure sufficient contact safety so that discomfort and skin injuries such as blisters and scratches are prevented. Skin injuries occur because of repetitive deformation of the skin tissue and slippage between the skin surface and the cuff, which connects the robot to the user [9]. Even in cases without injuries, skin deformation sometimes causes a feeling of discomfort.

The problem of pain and discomfort has been studied in the field of orthotics. Most of these studies evaluated the comfort of orthoses using subjective measures [10], [11]. Although some subjects in a previous study [12] attributed the discomfort to factors such as slip, it is difficult to determine each factor. On the other hand, several physical parameters were measured in some studies. Simon et al. used a pressure sensor and MRIs to evaluate the pain of the breast brace due to the increasing normal force [13]. The pressure under the contact area of a corset-type brace was also simulated in another study [14]. Esmaeili et al. quantified the relationship between the deformation energy of the skin and discomfort [15]. However, although the friction behavior around the contact surface generates an interaction force and causes skin deformation, the mechanism of this effect is not clearly understood because such deformation has not been measured previously. Especially, the uncertainty of the slip behavior disturbed to estimate the interaction force at the cuffs by measuring the displacement at the cuffs [16]. Thus, the risk of skin injuries and level of discomfort cannot be evaluated despite the existence of data on the physical strength of human tissues, which are shown below.

Some studies attempted to measure or estimate the contact between the cuff and skin. The difference between the knee joint mechanisms of a human and robot [17] causes a mismatch around the joint. Akiyama et al. estimated the relative displacement between the cuff and human thigh at the cuff position caused by this ergonomic mismatch. The interaction force measured at each cuff was related to the estimated displacement [7]. Another study analyzed the misalignment at the shoulder joint caused by a mechanical mismatch between a wearer and an upper-limb exoskeleton [18]. The displacement of the cuff due to misalignment at the elbow joint was also analyzed [19]. Although some of these studies measured the interaction force at the cuff, the actual skin deformation at the cuff was not measured.

Many current physical assistant robots measure only

Y. Akiyama, S.Okamoto, Y. Yamada and K. Ishiguro are with the Department of Mechanical Science and Engineering, Nagoya University, Nagoya, Aichi, Japan e-mail: akiyama-yasuhiro@mech.nagoya-u.ac.jp.

Manuscript received April 19, 2005; revised December 27, 2012.

the joint torque [20], [21], force [22], and ground reaction force [23] for achieving control and ensuring safety against fall risks. A safety mechanism for skin injuries cannot be devised using the joint torque, force, and limited motion range because the stress concentration and frictional force on the skin under the cuff might be overlooked because of uneven contact and the existence of local slippage.

Physical parameters of the human skin that affect the skin deformation and slippage were analyzed in earlier studies. For example, the viscoelasticity of human skin was measured under various conditions [24], [25], [26]. Some of these studies used a contactor with rotational motion whereas others used a contactor with linear motion to apply repetitive deformation to the skin. Some researchers [27], [28], [29] measured the friction coefficient along with other physical parameters. However, the friction coefficient of human skin easily changes in response to changes in environmental conditions such as humidity [30]. In addition, skin stretching was measured by measuring the strain of the skin between two fixation points [25], [26]. Such skin stretching was numerically analyzed by Tepole et al. [31]. A skin stretch model using a finite element method was developed to represent the nonlinear deformation of skin. Another group [32] measured not only the stretching of the skin surface but also the deformation occurring in the tissue under the skin. They reported that the range of skin deformation was less than 1 cm in the forearm. However, because of the slippage induced by a small normal force, the value of 1 cm does not represent the mechanical limit of the displacement between a cuff and human skin. Although these physical parameters can be used as basic data to analyze contact behavior, actual skin movement under an area covered by a wide object has not been analyzed and measured so far.

Thus, the direct measurement of friction behavior, including slippage, displacement, deformation, and interaction force and moment, around the cuff is required to understand the contact mechanism under the cuff. Lenzi et al. developed a sensor system that can measure the distribution of the normal force under the cuff using a distributed tactile sensor [33]. Although this sensor can detect the concentration of the vertical force, it cannot measure slippage and friction, which are crucial for assessing the risk of skin injuries. Ueda et al. developed a slip sensor which detects slip by measuring the vibration of the small needle which contacted to the surface [34]. Although this method could detect the slippage, it was difficult to know the amount of the slippage. Methods to monitor the slippage of the cuff are limited because the contact area is covered and skin is flexible. In addition, the use of some sensors can possibly change the surface condition of the cuff and make it difficult to monitor natural contact behavior. Therefore, a sensor that requires only a small contact area for measurement and can measure slippage without affecting the friction behavior is required. An optical method possibly meets this requirement because it potentially measures slippage without contact.

In this study, we installed optical slip sensors and force sensors on a cuff, which allows us to measure multiple types of contact information comprising the slippage, interaction force, and relative displacement between the cuff and human skin. Such measurements and analyses of contact behavior, including the direct measurement of slippage, can contribute to the development of a contact model that is useful for improving contact safety regulations.

II. Method

The experiment was performed with the permission of the institutional review board of Nagoya University.

A. Apparatus

A commercially available physical assistant robot[1] was used for the experiment without any actuation. Fig. 1 shows the configuration of the fixation and degrees of freedom of the robot. The cuff on the left thigh was replaced with a cuff in which two slip sensors and four force sensors were inserted (Fig. 2). Two two-dimensional imaging devices (ADNS-9500, Avago Technologies, Singapore) with lenses (ADNS-6190-002, Avago Technologies, Singapore) were supported by springs to ensure that there was no clearance between the sensors and the skin. Then, the surfaces of the cuff and springs were fixed to four three-axis force sensors (US06-H5, Tech Gihan Co., Ltd., Japan), which were placed on the base of the cuff. These force sensors were used to measure the interaction force and moment between the cuff and skin. The contact area of the cuff was 5.5 cm wide and 9.5 cm long. The structure of the modified cuff is shown in Fig. 3. The cuff was directly attached to the skin to avoid slippage between clothes and skin. The surface of the cuff was fixed on the lateral side of the human thigh which was parallel to the sagittal plane of the subject. The frequencies of measurement of the force and slippage were 50 Hz and 1 kHz, respectively. The slip sensor measured the position in the Cartesian system, and the resolution of the slip sensor was 0.06 mm.

The posture of the subject and the relative motion between the subject and the robot were measured using a three–dimensional motion capture system (MAC 3D system, Motion Analysis Corporation, CA), the outputs from which were sampled at 100 Hz. Markers were attached to the lateral side of the center of the hip, knee, and ankle joint of the robot, and the knee and ankle joint of the subject. The data for the hip joint of the subject were determined from the markers that were attached to the sacral and anterior superior iliac points on the spine [35]. The posture and position of the pelvis of the subject were calculated from the same markers, whereas those of the robot were measured using markers attached to the pelvis link. The positions of the cuff were marked on the lateral side of the robotic link. The positions covered by the robot were determined using cluster markers.

[1]Because of contractual obligations aimed at preventing the evaluation of this robot, the name, manufacturer, and details of the assist algorithm cannot be revealed.

This article has been accepted for publication in a future issue of this journal, but has not been fully edited. Content may change prior to final publication. Citation information: DOI 10.1109/TNSRE.2015.2464719, IEEE Transactions on Neural Systems and Rehabilitation Engineering

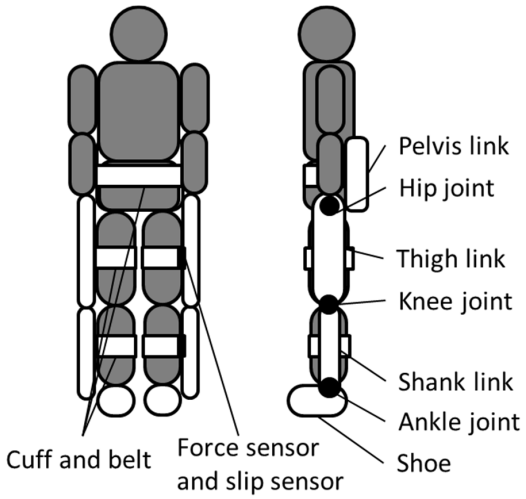

Fig. 1. Overview of physical assistant robot

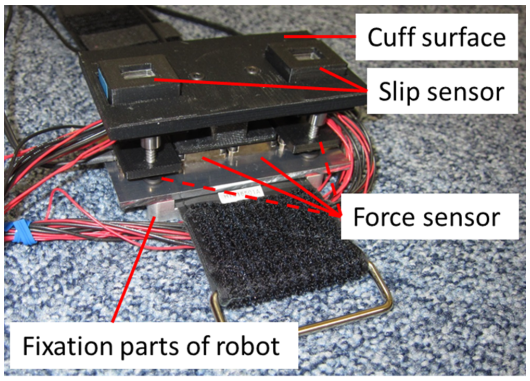

Fig. 2. Instrumented cuff of left thigh

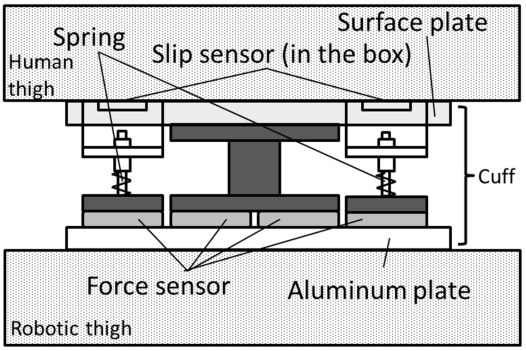

Fig. 3. Structure of instrumented cuff

B. Protocol

Ten healthy male volunteers participated in the experiment. They were between 21 and 24 years of age (average age: 22.3 years) and between 169 and 178 cm in height (average height: 173.0 cm). After attaching the robot to the subject, the length of the thigh and shank links was adjusted to align the subject's hip and knee joints to those of the robot. Then, the cuffs were fixed to the legs using belts. The belts were tightened as firmly as possible without causing discomfort to the subject. Before recording was started, several minutes were spent on adaptation. During adaptation, the subject attempted sit-down and stand-up motions continuously until he became comfortable.

In the experiment, the subject repeated sit-down and stand-up motions on a 52-cm-tall chair more than 15 times. The sit-to-stand motion was selected for this experiment because it is the fundamental motion performed in daily activities and might require the assistance of a physical assistant robot. This motion has been studied previously, and most of its characteristics are known [36], [37].

C. Data Processing

The positions of the markers attached to the center of joints of the subject and robot were projected on to the sagittal plane in which the sit-to-stand motion occurred. Then, the posture and position of the subject and robot were defined using body links, each of which was defined as the line connecting two adjacent joint centers. Then, the relative displacement of the cuff position on the skin surface was calculated by comparing the position of the cuff and its initial position on the human thigh, which was marked as a particular point between the hip and knee joints. This relative displacement includes the slippage and deformation of the skin tissue because of the friction behavior. Although surface slippage could be obtained from the slip sensor, skin deformation, which includes shear deformation and inner slippage of the tissue, was estimated indirectly. The interaction force was obtained by the summation of the outputs from all force sensors. All data were filtered using a linear-phase finite-impulse-response low-pass filter with a cutoff frequency of 2 Hz and a filter order of 30.

The geometry of the robot, cuff, and human subject is shown in Fig. 4. At the thigh cuff, slip sensors were arrayed in tandem in the longitudinal direction of the robotic thigh link, which was defined as the line connecting the center of the hip and knee joints. Because the position of the cuff was measured at the center of the slip sensors, the relative displacement at each slip sensor was calculated from the relative position and attitude of the cuff as follows:

$$\begin{aligned} \boldsymbol{d_{s1}}(t) &= \boldsymbol{D_t}(t) + \big(l\sin(\theta_d(t)), -l(1-\cos(\theta_d(t)))\big) \\ \boldsymbol{d_{s2}}(t) &= \boldsymbol{D_t}(t) + \big(-l\sin(\theta_d(t)), l(1-\cos(\theta_d(t)))\big) \end{aligned} \tag{1}$$

where θ_d is the relative angle between the thigh link of the robot and the human thigh. l is the distance between the slip sensor and center of the cuff. $\boldsymbol{D_t}$, $\boldsymbol{d_{s1}}$, and $\boldsymbol{d_{s2}}$ are the relative displacements between the cuff and human thigh and are defined in the X–Y coordinate system. The Y–axis corresponds to the direction of the longitudinal axis of the robotic thigh. The original points of each coordinate were considered as the position of the cuff center or slip sensors. The first term of (1) represents the translational motion of the cuff, and the second term represents the rotational motion.

This article has been accepted for publication in a future issue of this journal, but has not been fully edited. Content may change prior to final publication. Citation information: DOI 10.1109/TNSRE.2015.2464719, IEEE Transactions on Neural Systems and Rehabilitation Engineering

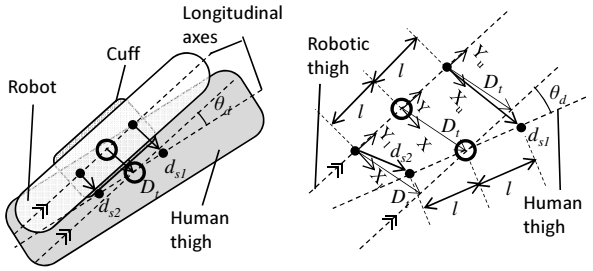

Fig. 4. Coordination system around thigh cuff (left: overview, right: definitions of parameters)

TABLE I
AVERAGE DURATION OF SIT-TO-STAND MOTION FOR EACH SUBJECT

Subject no.	Sitting pace [s]	± SD	Standing pace [s]	± SD
1	1.4	0.1	1.3	0.1
2	1.5	0.2	1.4	0.1
3	1.7	0.2	1.2	0.1
4	1.8	0.4	1.5	0.1
5	1.5	0.1	1.3	0.1
6	2.3	0.2	2.0	0.1
7	1.7	0.2	1.6	0.1
8	3.1	0.2	2.6	0.2
9	2.2	0.1	1.7	0.1
10	1.4	0.1	1.2	0.1

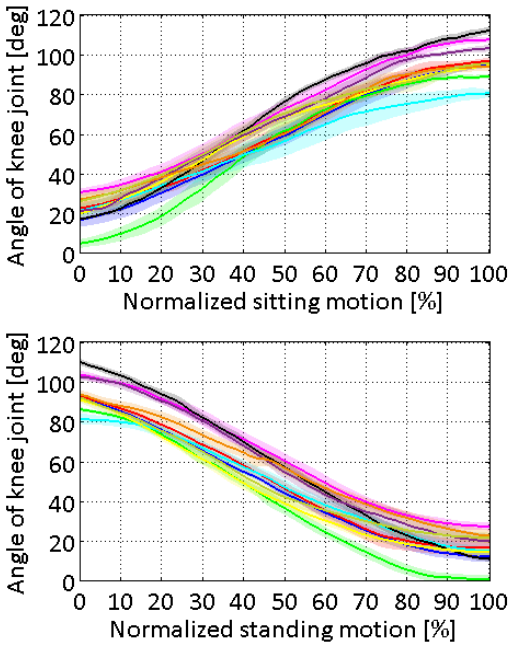

Fig. 5. Averages and standard deviations of θ_k for each subject during sitting (top) and standing (bottom) phases

Among all the sit-to-stand motions, the first five motions of each subject were not used because of the instability of the contact condition around the cuff. The next 10 motions were analyzed. Motions were separated into two phases: sitting phase and standing phase. The static phase, in which the motions were not measured, was not used for the analysis. The angle of the knee joint of the subject was used to separate the phases. All the separated data were normalized by the period of each phase for comparison between subjects.

III. RESULTS

A. Posture of Subjects

The average durations of the sit-to-stand motions of each subject are listed in Table I. Despite the differences between the motion paces of the subjects, the deviations within the paces of a subject were small, which suggested the stability of motions of almost all the subjects. Fig. 5 shows the change in the knee angle (θ_k) for each subject. These changes are very similar to those observed in the case of the sit-to-stand motion of a healthy person [38], indicating that the motions were normal even when the robot was worn.

The postures of the representative subject and robot are plotted in Fig. 6. In this experiment, the robot was located marginally anterior to the aligned position of the subject to fit the cuff to the skin. However, the relative position of the robot changed during the sit-to-stand motion because of the deformation and slippage of the fixation parts.

The largest displacement of the cuff position between the subject and robot was observed around the middle phase of the sitting motion. During this phase, the subject's thigh pulled the robotic thigh and the human motion preceded the robotic motion. Then, in the late sitting phase, the robot lowered itself under the effect of gravity.

B. Displacement

The relative displacement which includes the slippage and skin deformation at the cuff is the basic parameter representing the motion around the cuff. Figs. 7–10 show the relative displacement along the long and short axes in the sagittal plane. Although the magnitudes of the displacement differ individually, especially in the sitting posture, the displacement trend is common across subjects. As shown in Fig. 7, during the sitting phase, the relative displacement in the **X** direction increases initially, and the peak is reached at around 50% of the sitting phase. Then, the displacement decreases until the end of the sitting motion. The range of the displacement during the sitting phase is approximately 20–70 mm. As shown in Fig. 8, the displacement returns to zero gradually until the end of the standing phase. The displacement in the **Y** direction also increases up to the 60–80% of the sitting phase, and it slightly decreases in the late sitting phase (Fig.9). The peak displacement along the **Y** direction is approximately 5–40 mm in this phase. In the standing phase as well, the displacement in the **Y** direction decreases gradually (Fig. 10).

Along both axes, there are large individual differences. The range of the relative displacement differs up to a maximum of 50 mm between the orange and yellow lines along the short (**X**) axis (Fig. 7) and 25 mm between the black and purple lines along the long (**Y**) axis (Fig. 9).

This article has been accepted for publication in a future issue of this journal, but has not been fully edited. Content may change prior to final publication. Citation information: DOI 10.1109/TNSRE.2015.2464719, IEEE Transactions on Neural Systems and Rehabilitation Engineering

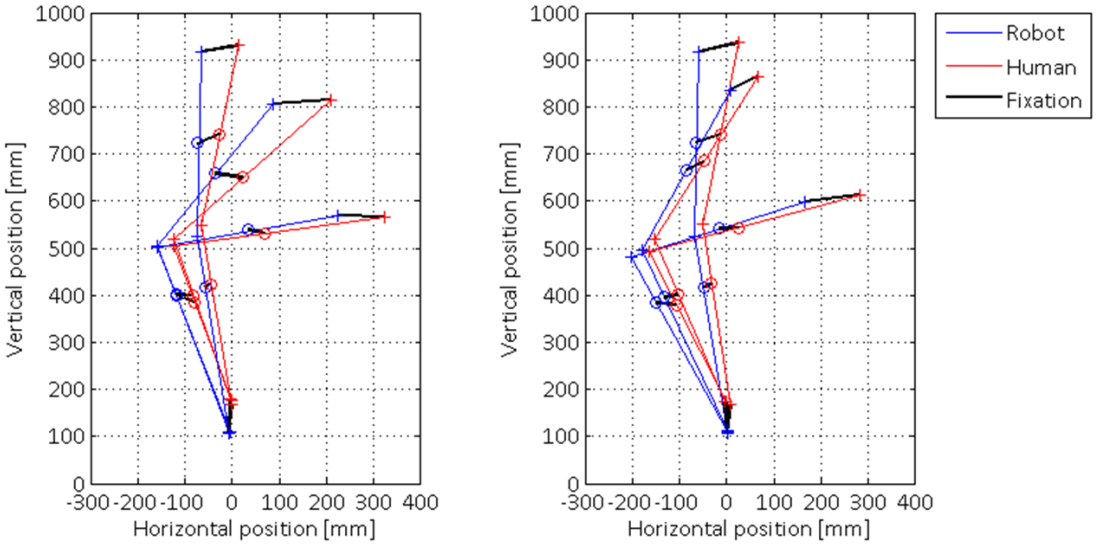

Fig. 6. Postures of human and robot (left: sitting, right: standing)

Another feature of the displacement in the **X** direction was the difference in the displacement between sensors. The displacement at the position of the upper sensor was always larger than that at the position of the lower sensor. This trend indicated the unevenness of the displacement under the cuff.

One of the reasons for the difference in the relative displacement between sensors in the **X** direction was the rotation of the human thigh link against the robotic thigh (Fig. 11). Because of the rotation, the relative displacement at the position of the upper sensor was larger than that at the position of the lower sensor by approximately 10 mm.

The direction of the displacement suggested that the thigh link of the robot moved downward and backward with respect to the subject in the sitting phase. According to Fig. 9, the position of the robot dropped rapidly at around 50% of the sitting phase. Then, the relative displacement gradually returned to zero in the standing phase. In contrast, Fig. 8 shows that the displacement in the **X** direction did not converge to zero in the standing phase. This mismatch between the end of the standing phase and the beginning of the sitting phase implies that the residual displacement was canceled by the subject in the standing posture before starting the next motion. In addition, the standard deviation was larger along the short axis (**X**) than along the long axis (**Y**) because of the large displacement of the hip fixation in the front-back direction.

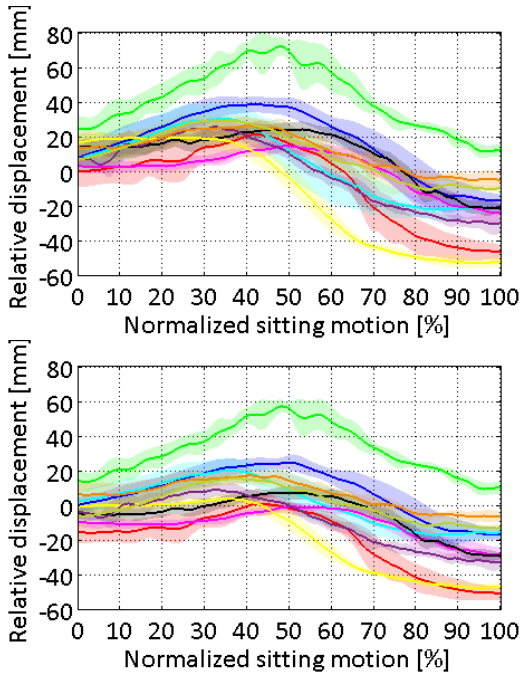

Fig. 7. Relative displacement in **X** direction between human and robot in sitting phase (top: upper sensor, bottom: lower sensor)

C. Slippage

The amount of slippage in the **X** and **Y** directions is presented in Figs. 12–15. For some subjects, the maximum slippage reached several millimeters, whereas for others, the slippage was negligible at the position of the lower slip sensor. The slippage differed between sensor positions in addition to the subjects, phases, and axes, which suggested that the slippage included both translational and rotational movements. The difference in the slippage between sensors was less in the **Y** direction than in the **X** direction given that the rotation center of the slippage was located near the knee joint. Because the slip sensors were aligned to the longitudinal axis of the thigh link, the effect of cuff rotation seldom affected the slippage in the **Y** direction. The difference in slippage in the **Y** direction represented

This article has been accepted for publication in a future issue of this journal, but has not been fully edited. Content may change prior to final publication. Citation information: DOI 10.1109/TNSRE.2015.2464719, IEEE Transactions on Neural Systems and Rehabilitation Engineering

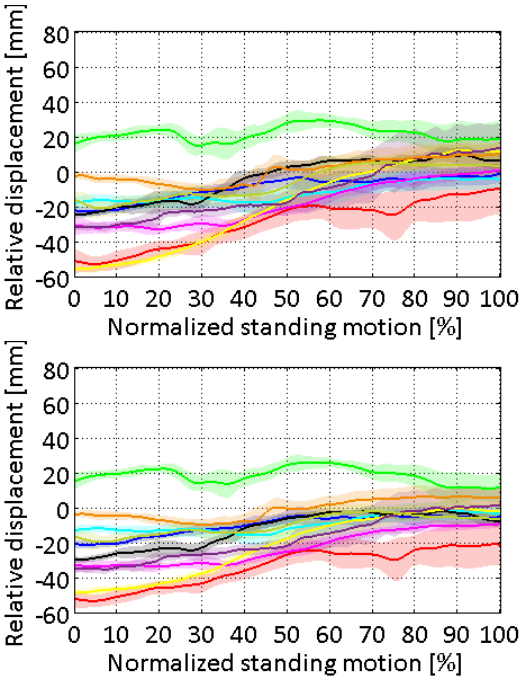

Fig. 8. Relative displacement in **X** direction between human and robot in standing phase (top: upper sensor, bottom: lower sensor)

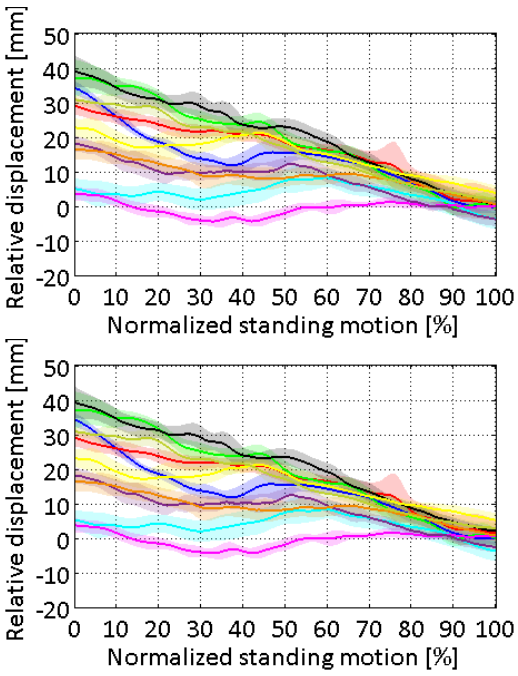

Fig. 10. Relative displacement in **Y** direction between human and robot in standing phase (top: upper sensor, bottom: lower sensor)

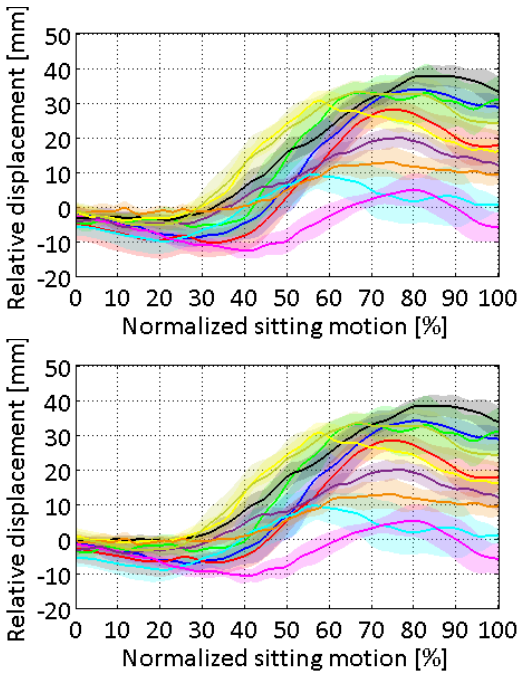

Fig. 9. Relative displacement in **Y** direction between human and robot in sitting phase (top: upper sensor, bottom: lower sensor)

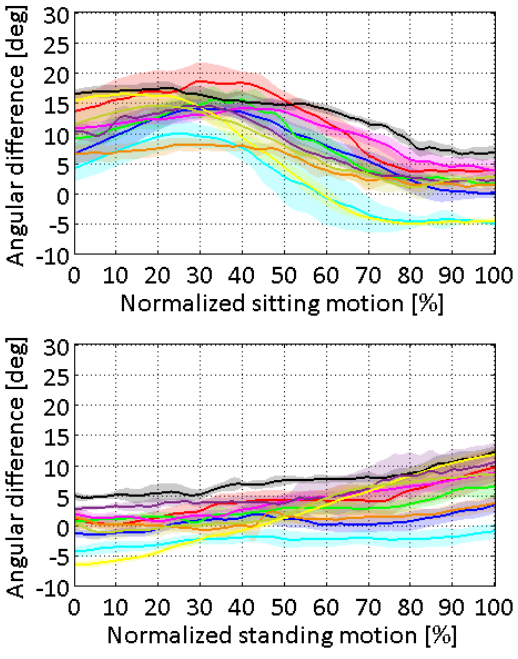

Fig. 11. Angular difference between thigh links (top: sitting, bottom: standing)

the skin stretching between the sensors.

In contrast, the difference in the slippage in the **X** direction suggested the existence of rotation, local slip, and skin movement. Especially, during the sitting phase, the slippage measured by the upper sensor along the **X**-axis was notably larger than that measured by the lower sensor along the **X**-axis (Fig. 12). This trend corresponded to the trend of the relative displacement. For one subject, the slippage was notably large, in terms of not only the amount but also the deviation. Such instability and uniqueness suggested that individual differences should be carefully considered when the slip behavior is generalized.

This article has been accepted for publication in a future issue of this journal, but has not been fully edited. Content may change prior to final publication. Citation information: DOI 10.1109/TNSRE.2015.2464719, IEEE Transactions on Neural Systems and Rehabilitation Engineering

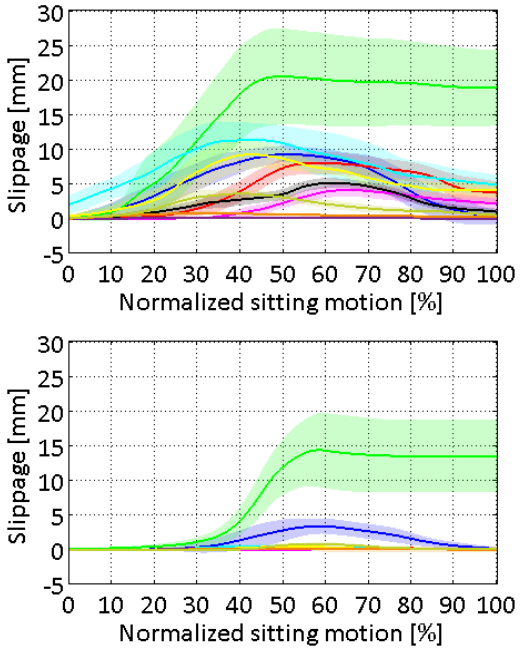

Fig. 12. Slippage in **X** direction between human and robot in sitting phase (top: upper sensor, bottom: lower sensor)

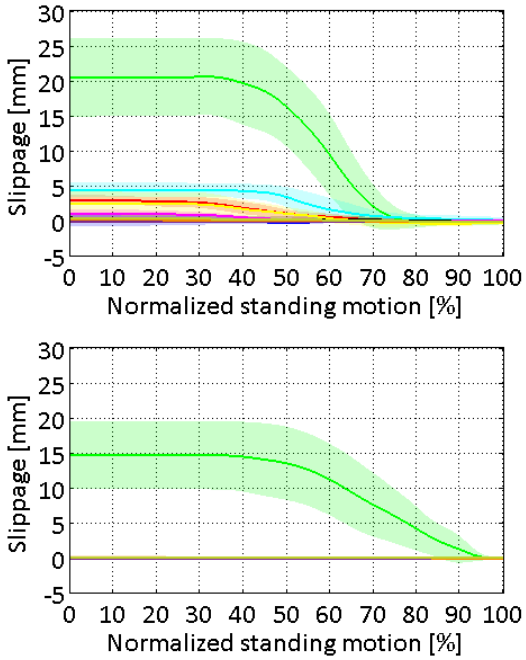

Fig. 13. Slippage in **X** direction between human and robot in standing phase (top: upper sensor, bottom: lower sensor)

Although such large individuality existed, a common trend could be found. Around the middle phase of the sitting motion, slip occurred in both the **X** and **Y** directions. The direction of slippage suggested that the robot slid downward and backward, which corresponded to the direction of the relative displacement. However, slippage in the **Y** direction eased at the end of the sitting phase (Fig. 14) and it had no apparent relationship with the change in the relative displacement.

D. Interaction force and moment

Interaction force and moment were generated at the cuff because of the motion of the subjects. Although the interaction force in the compression direction, normal to the skin surface, affects the comfort of the subject, the amount of shear force is more important to evaluate the risk of skin injuries [9]. Thus, the discussion in this study focuses on the sagittal plane. Figs. 16 and 17 show the change in the interaction force. The interaction moment is shown in Fig. 18. In Figs. 16 and 18, data for one subject were omitted because of an electronic fault in the sensor used for force measurements in the **X** direction.

The change in the interaction force in the **X** direction (Fig. 16) and the interaction moment (Fig. 18) was nearly flat with small peaks in the middle sitting phase. A few participants, represented by green and ocher curves, were exceptions. The trend in the **Y** direction differed from that in the **X** direction. One prominent peak was found in the middle of both the sitting and standing phases (Fig. 16).

Figs. 16–18 also show that two among the ten subjects were found to be very unique. The patterns of the force and moment of the two subjects,represented by ocher

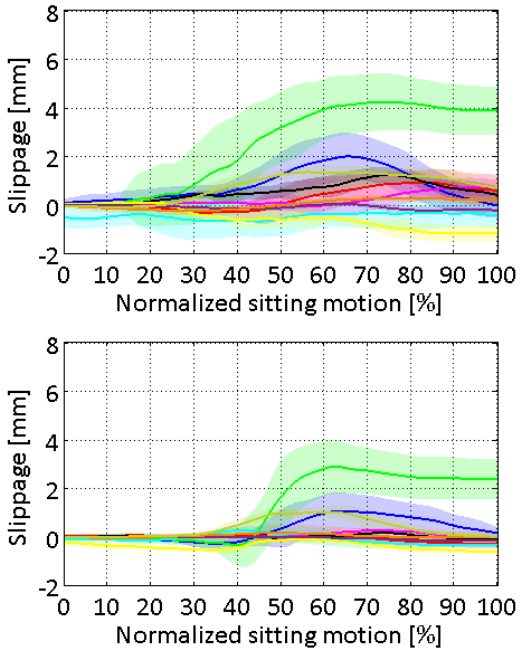

Fig. 14. Slippage in **Y** direction between human and robot in sitting phase (top: upper sensor, bottom: lower sensor)

and green lines, differed from those of the other subjects. Especially, for these two subjects, the force in the **X** direction and the moment drastically changed during the motions. In addition, each subject had different offsets of the interaction force and moment in the standing posture, which might be attributed to the initial condition of

This article has been accepted for publication in a future issue of this journal, but has not been fully edited. Content may change prior to final publication. Citation information: DOI 10.1109/TNSRE.2015.2464719, IEEE Transactions on Neural Systems and Rehabilitation Engineering

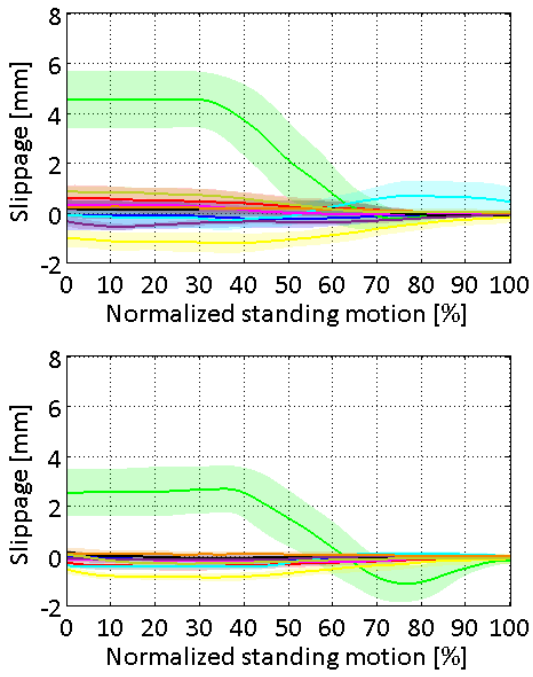

Fig. 15. Slippage in **Y** direction between human and robot in standing phase (top: upper sensor, bottom: lower sensor)

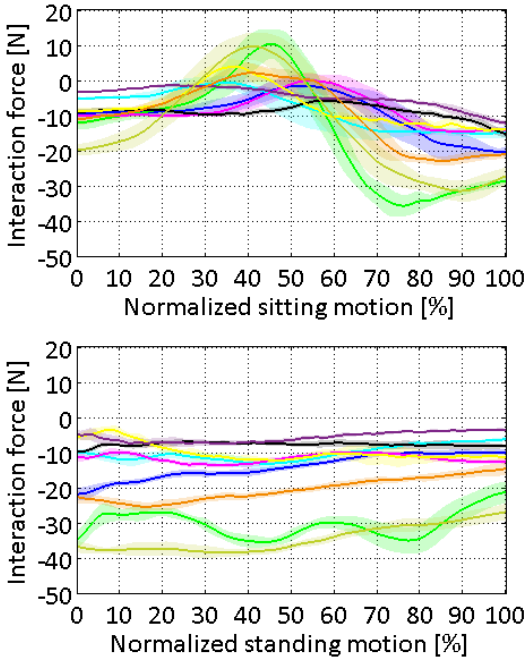

Fig. 16. Interaction force in **X** direction between human and robot at thigh cuff (top: sitting, bottom: standing)

fixation of the cuff. When tightening the cuff belts, several degrees of initial force were inevitably applied.

IV. Discussion: Contact behavior around the cuff and risks of skin injuries

A. General Behavior

The motion and force in the contact area of the thigh cuff were measured using various sensors, and the relative motion, slippage, and interaction force and moment were compared with each other. In general, these parameters changed in the same direction during the major part of the motions. This was because the kinematic mismatch changed the trajectories of the thighs of the human and robot, and this relative displacement interacted with the force, moment, and slippage through physical parameters such as the friction coefficient and viscoelastic constant.

The measured slippage values in the **X** direction were different between the two slip sensors, whereas their general profiles were similar. This difference suggested the existence of an uneven distribution of slippage beneath the cuff due to partial slip and rotation. During the sit-to-stand motion, slippage was larger at the position of the upper sensor than at the position of the lower sensor in the **X** direction. This tendency could be attributed to the rotation of the thigh link. The change in the rotation angle and moment also supported this tendency. Because of the relative rotation, the position that was close to the hip joint showed large movement, which indicated a high risk of injuries.

An important inference from the comparison between slippage and relative displacement was that a maximum of 40 mm of the actual relative displacement, which was calculated by subtracting slippage (Figs. 12 and 14) from relative displacements (Figs. 7 and 9), seemed too large to be considered as skin stretching. This gap was probably caused by the deformation of skin, fat, and muscle tissues. During joint bending, skin around the joint was deformed because of the change in its shape and because of tension. This large deformation around the joint propagated to the skin and tissue of the thigh. The flabbiness of the skin and tissue movement affected the relative displacement. Thus, the results of this experiment indicated that not only the relative displacement and the slippage of the skin surface but also the deformation of the skin and tissue caused by motion changed the risk of skin injuries.

According to the changes in the interaction force (Figs. 16 and 17), the shear stress was approximately 0.4×10^4 Pa when considering the contact area. Although this value was ten times smaller than the stress required to generate a blister [30], the unevenness of the contact indicated the probability of stress concentration. Thus, safety margins should include the effect of such stress concentration.

B. Individuality

The results for all parameters such as the displacement, slippage, and interaction force and moment differed drastically for each subject. Such individuality appeared especially in the sitting posture. Thus, individuality increased in the sitting phase and converged in the standing phase.

Among all the subjects, one subject, represented by the green line, had a large relative displacement and slippage.

This article has been accepted for publication in a future issue of this journal, but has not been fully edited. Content may change prior to final publication. Citation information: DOI 10.1109/TNSRE.2015.2464719, IEEE Transactions on Neural Systems and Rehabilitation Engineering

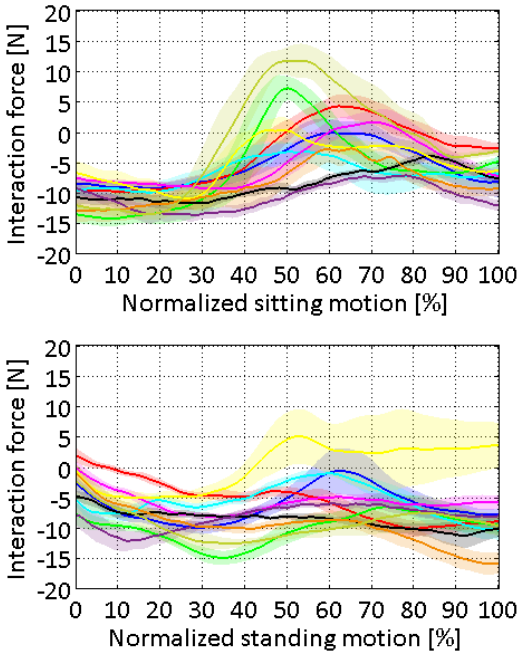

Fig. 17. Interaction force in **Y** direction between human and robot at thigh cuff (top: sitting, bottom: standing)

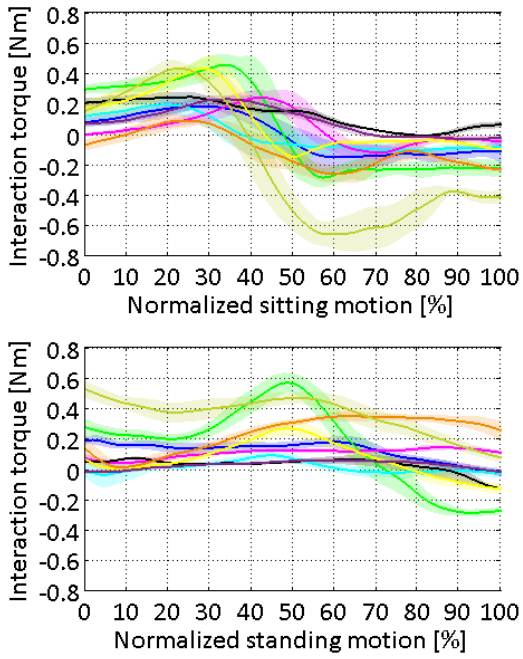

Fig. 18. Interaction moment in **X**–**Y** plane between human and robot at thigh cuff (top: sitting, bottom: standing)

Unlike the other subjects, for this subject, the slippage occurring during the middle of the sitting phase did not decrease at the end of the sitting phase (Figs. 12 and 14) and it continued until the middle of the standing phase (Figs. 13 and 15). In addition, the interaction force and moment became large when a large slippage occurred in the middle of the sitting phase (Figs. 16 to 18). This simultaneous increase in the slippage, the interaction force, and moment indicated the deformation of the skin and tissue. This potentially indicated the stacking of the skin and tissue, which meant the elevation of skin tissue, at the edge of the cuff in the middle of the sitting phase. The stacking increases the maximum shear force during the motion, thus increasing the risk of skin injuries. The observation of the interaction force and skin deformation around the edge of the cuff could be used to determine whether such phenomena occur.

In addition, the contact behavior of another subject, represented by the ocher line, was differed from that of the subject represented by the green line. The amount of slippage represented by the ocher line was not large in the **X** direction despite the interaction force and moment for this subject being larger than those for the other subjects. This difference might have originated from individual differences in physical parameters such as the friction coefficient and viscoelasticity. This kind of individuality in skin conditions is also likely to influence the risks of skin injuries.

V. Conclusion

In this study, the contact behavior of the cuff, including the slippage at the thigh cuff, was analyzed. The results suggested that the difference between the motions of the human and robot interacted with the relative displacement, the interaction force and moment, and the slippage at the cuff. For the first time, the measurement of the slippage enabled us to separate the relative displacement to the deformation of the tissue and slippage of the skin. During the sit-to-stand motions, on average, several millimeters of slippage and approximately 40 millimeters of the displacement of the cuff were measured with the interaction forces and moment between the cuff and human thigh being approximately 10 N and 0.2 N·m.

Acknowledgment

This study was conducted as a part of the "Practical Applications of Service Robot Project," which is directed by the New Energy and Industrial Technology Development Organization (NEDO). Also, we thank the support by JSPS KAKENHI Grant Number 26750121.

References

[1] S. Kubota, Y. Nakata, K. Eguchi, H. Kawamoto, K. Kamibayashi, M. Sakane, Y. Sankai, and N. Ochiai, "Feasibility of rehabilitation training with a newly developed wearable robot for patients with limited mobility," *Archives of Physical Medicine and Rehabilitation*, vol. 94, pp. 1080–1087, 2013.

[2] J. Hidler, D. Nichols, M. Pelliccio, K. Brady, D. D. Campbell, J. H. Kahn, and T. G. Hornby, "Multicenter randomized clinical trial evaluating the effectiveness of the lokomat in subacute stroke," *Neurorehabil Neural Repair*, vol. 23, no. 1, pp. 5–13, 2009.

[3] K. Yasuhara, K. Shimada, T. Koyama, T. Ido, K. Kikuchi, and Y. Endo, "Walking assist devices with stride management system," *Honda R&D Technical Review*, vol. 21, no. 2, pp. 54–62, 2009.

[4] H. Kobayashi, T. Aida, and T. Hashimoto, "Muscle suit development and factory application," *International Journal of Automation Technology*, vol. 3, no. 6, pp. 709–715, 2009.
[5] T. Kusaka, T. Tanaka, S. Kaneko, Y. Suzuki, M. Saito, and H. Kajiwara, "Assist force control of smart suit for horse trainers considering motion synchronization," *International Journal of Automation Technology*, vol. 3, no. 6, pp. 723–730, 2009.
[6] A. B. Zoss, H. Kazerooni, and A. Chu, "Biomechanical design of the berkeley lower extremity exoskeleton (BLEEX)," *IEEE/ASME Transactions on mechatronics*, vol. 11, no. 2, pp. 128–138, April 2006.
[7] Y. Akiyama, Y. Yamada, K. Ito, S. Oda, S. Okamoto, and S. Hara, "Test method for contact safety assessment of a wearable robot -analysis of load caused by a misalignment of the knee joint-," in *The 21st IEEE International Symposium on Robot and Human Interactive Communication*, September 2012, pp. 539–544.
[8] ISO, "Robots and robotic devices – safety requirements for personal care robots," International Organization for Standardization, Tech. Rep. ISO 13482:2014, 2014.
[9] P. F. D. Naylor, "Experimental friction blisters," *British Journal of Dermatology*, vol. 67, no. 10, pp. 327–342, 1955.
[10] T. J. Lane, K. B. Landorf, D. R. Bonanno, A. Raspovic, and H. B. Menz, "Effects of shoe sole hardness on plantar pressure and comfort in older people with forefoot pain," *Gait and Posture*, no. 39, pp. 247–251, 2014.
[11] A. Marchini, S. Lauermann, M. Minetto, G. Massazza, and N. Maffiuletti, "Differences in proprioception, muscle force control and comfort between conventional and new-generation knee and ankle orthoses," *Journal of Electromyography and Kinesiology*, vol. 24, pp. 437–444, 2014.
[12] T. Schmalz, E. Knopf, H. Drewitz, and S. Blumentritt, "Analysis of biomechanical effectiveness of valgus-inducing knee brace for osteoarthritis of knee," *Journal of Rehabilitation Research and Development*, vol. 47, no. 5, pp. 419–430, 2010.
[13] S. Armstrong, K. Ried, A. Sali, and P. McLaughlin, "A new orthosis reduces pain and mechanical forces in prone position in women with augmented or natural breast tissue: A pilot study," *Journal of Plastic, Reconstructive and Aesthetic Surgery*, vol. 66, pp. 179–188, 2013.
[14] N. Cobetto, C.-E. Aubin, J. Clin, S. L. May, F. Desbiens-Blais, H. Labelle, and S. Parent, "Braces optimized with computer-assisted design and simulations are lighter, more comfortable, and more efficient than plaster-cast braces for the treatment of adolescent idiopathic scoliosis," *Spine Deformity*, vol. 2, pp. 276–284, 2014.
[15] M. Esmaeili, K. Gamage, E. Tan, and D. Campolo, "Ergonomic considerations for anthropomorphic wrist exoskeletons: a simulation study on the effects of joint misalignment," in *2011 IEEE/RSJ International Conference on Intelligent Robots and Systems*, 2011, pp. 4905–4910.
[16] Y. Akiyama, Y. Yamada, and S. Okamoto, "Interaction forces beneath cuffs of physical assistant robots and their motion-based estimation," *Advanced Robotics*, p. [DOI] 10.1080/01691864.2015.1055799, 2015.
[17] G. T. Yamaguchi and F. E. Zajac, "A planar model of the knee extensor mechanism," *Journal of Biomechanics*, vol. 22, no. 1, pp. 1–10, 1989.
[18] A. Schiele and F. C. T. van der Helm, "Kinematic design to improve ergonomics in human machine interaction," *IEEE Transactions on Neural Systems and Rehabilitation Engineering*, vol. 14, no. 4, pp. 456–469, 2006.
[19] N. Jarrassé and G. Morel, "Connecting a human limb to an exoskeleton," *IEEE Transactions on Robotics*, vol. 28, no. 3, June 2012.
[20] T. Hayashi, H. Kawamoto, and Y. Sankai, "Control method of robot suit hal working as operator's muscle using biological and dynamical information," in *2005 IEEE/RSJ International Conference on Intelligent Robots and Systems*, August 2005, pp. 3063–3068.
[21] C. L. Lewis and D. P. Ferris, "Invariant hip moment pattern while walking with a robotic hip exoskeleton," *Journal of Biomechanics*, vol. 44, pp. 789–793, 2011.
[22] D. Zanotto, T. Lenzi, P. Stegall, and S. K. Agrawal, "Improving transparency of powered exoskeletons using force/torque sensors on the supporting cuffs," in *2013 IEEE International Conference on Rehabilitation Robotics*, June 2013, pp. 1–6.
[23] V. Krishnamoorthy, W.-L. Hsu, T. M. Kesar, D. L. Benoit, S. K. Banala, R. Perumal, V. Sangwan, S. A. Binder-Macleod, S. K. Agrawal, and J. P. Scholz, "Gait training after stroke: A pilot study combining a gravity-balanced orthosis, functional electrical stimulation, and visual feedback," *Journal of Neurologic Physical Therapy*, vol. 32, pp. 192–202, December 2008.
[24] R. O. Potts, J. Dan A. Chrisman, and J. Edmund M. Buras, "The dynamic mechanical properties of human skin in vivo," *Journal of Biomechanics*, vol. 16, no. 6, pp. 365–372, 1983.
[25] J. A. Clark, J. C. Y. Cheng, and K. S. Leung, "Mechanical properties of normal skin and hypertrophic scars," *Burns*, vol. 22, no. 6, pp. 443–446, 1996.
[26] D. Bader and P. Bowker, "Mechanical characteristics of skin and underlying tissues in vivo," *Biomaterials*, vol. 4, pp. 305–308, 1983.
[27] M. Aso, Y. Yamada, K. Yoshida, Y. Akiyama, and Y. Ito, "Evaluation of the mechanical characteristics of human thighs for developing complex dummy tissues," in *2013 IEEE International Conference on Robotics and Biomechanics*, December 2013, pp. 1450–1455.
[28] A. F. EL-SHIMI, "In vivo skin friction measurements," *Journal of the Society of Cosmetic Chemists*, vol. 28, no. 2, pp. 37–51, 1977.
[29] J. E. Sanders, J. M. Greve, S. B. Mitchell, and S. G. Zachariah, "Material properties of commonly-used interface materials and their static coefficients of friction with skin and socks," *Journal of Rehabilitation Research and Development*, vol. 35, no. 2, pp. 161–176, 2014.
[30] P. F. D. Naylor, "The skin surface and friction," *British Journal of Dermatology*, vol. 67, no. 7, pp. 239–246, Jul 1955.
[31] A. B. Tepole, A. K. Gosain, and E. Kuhl, "Stretching skin: The physiological limit and beyond," *International Journal of Non-Linear Mechanics*, vol. 47, pp. 938–949, 2012.
[32] M. Kwiatkowska, S. Franklin, C. Hendriks, and K. Kwiatkowski, "Friction and deformation behaviour of human skin," *Wear*, vol. 267, pp. 1264–1273, 2009.
[33] T. Lenzi, N. Vitiello, S. M. M. D. Rossi, A. Persichetti, F. Giovacchini, S. Roccella, F. Vecchi, and M. C. Carrozza, "Measuring human-robot interaction on wearable robots: A distributed approach," *Mechatronics*, vol. 21, pp. 1123–1131, 2011.
[34] M. Ueda, K. Iwata, and H. Shingu, "Tactile sensors for industrial robot to detect slip," in *2nd International Symposium on Industrial Robots*, May 1972, pp. 63–76.
[35] A. L. Bell, D. R. Pedersen, and R. A. Brand, "A comparison of the accuracy of several hip center location prediction methods," *Journal of Biomechanics*, vol. 23, no. 6, pp. 617–621, 1990.
[36] D. S. Reisman, J. P. Scholz, and G. Schöner, "Differential joint coordination in the tasks of standing up and sitting down," *Journal of Electromyography and Kinesiology*, vol. 12, pp. 493–505, 2002.
[37] G. D. Baer and A. M. Ashburn, "Trunk movements in older subjects during sit-to-stand," *Archives of Physical Medicine and Rehabilitation*, vol. 76, pp. 844–849, 1995.
[38] A. Kralj, R. J. Jaeger, and M. Munih, "Analysis of standing up and sitting down in humans: Definitions and normative data presentation," *Journal of Biomechanics*, vol. 23, no. 11, pp. 1123–1138, 1990.

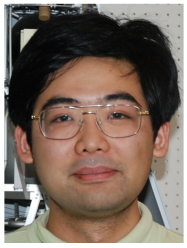

Yasuhiro Akiyama Yasuhiro Akiyama received the B.E. degree in engineering from Tokyo Institute of Technology, Tokyo, Japan, in 2006, and the M.S. and the Ph.D. degree in engineering from the University of Tokyo, Tokyo, Japan, in 2008 and 2011, respectively. Since then, he has been a postdoctoral researcher at Nagoya University, Nagoya, Japan. His main areas of research interests are mechanical safety, human-robot interaction, and manned space mission.

Shogo Okamoto Shogo Okamoto received MS and PhD degrees in information sciences in 2007 and 2010, respectively, from the Graduate School of Information Sciences, Tohoku University. Since 2010, he has been an assistant professor at the Graduate School of Engineering, Nagoya University. His research interests include haptics and human-assistive technology.

Yoji Yamada YAMADA, Yoji received a doctor degree from Tokyo Institute of Technology in 1990. He had been with Toyota Technological Institute since 1983 and became an associate professor in the Graduate School of the Institute. In 2004, he joined Intelligent Systems Research Institute of National Institute of Advanced Industrial and Science Technology (AIST). In 2009, he moved to the Department of Mechanical Science and Engineering, Graduate School of Engineering, Nagoya Unversity as a professor. His current research interests include safety and intelligence technology in human/ machine systems, their robotic sensing and control.

Kenji Ishiguro Kenji Ishiguro received the M.S. degree in engineering from Nagoya University, in 2014. Since then, he has been working for DENSO Corporation as an engineer. Kenji Ishiguro received the B.E. and M.S. degree in engineering from Nagoya University, in 2012 and 2014, respectively. Since then, he has been working for DENSO Corporation as an engineer. His research interests are human-robot interaction, wearable robotics, and mechanical safety.